Proc. Natl. Acad. Sci. USA
Vol. 93, pp. 10034–10039, September 1996
Biochemistry

Structure and inhibition of plasmepsin II, a hemoglobin-degrading enzyme from *Plasmodium falciparum*

(malaria/drug design/crystallography/aspartic protease/cathepsin D)

A. M. SILVA*, A. Y. LEE*, S. V. GULNIK*, P. MAJER*, J. COLLINS*, T. N. BHAT*, P. J. COLLINS*, R. E. CACHAU*, K. E. LUKER†, I. Y. GLUZMAN†, S. E. FRANCIS†, A. OKSMAN†, D. E. GOLDBERG†, AND J. W. ERICKSON*

*Structural Biochemistry Program, National Cancer Institute/SAIC, P.O. Box B, Frederick, MD 21702; and †Howard Hughes Medical Institute, Departments of Molecular Microbiology and Medicine, and The Jewish Hospital of St. Louis, Washington University School of Medicine, Box 8230, 660 South Euclid Avenue, St. Louis, MO 63110

Communicated by David Davies, National Institute of Diabetes and Digestive and Kidney Diseases, Bethesda, MD, May 21, 1996 (received for review March 6, 1996)

ABSTRACT **_Plasmodium falciparum_ is the major causative agent of malaria, a disease of worldwide importance. Resistance to current drugs such as chloroquine and mefloquine is spreading at an alarming rate, and our antimalarial armamentarium is almost depleted. The malarial parasite encodes two homologous aspartic proteases, plasmepsins I and II, which are essential components of its hemoglobin-degradation pathway and are novel targets for antimalarial drug development. We have determined the crystal structure of recombinant plasmepsin II complexed with pepstatin A. This represents the first reported crystal structure of a protein from *P. falciparum*. The crystals contain molecules in two different conformations, revealing a remarkable degree of interdomain flexibility of the enzyme. The structure was used to design a series of selective low molecular weight compounds that inhibit both plasmepsin II and the growth of *P. falciparum* in culture.**

Malaria, a disease caused by parasites of the genus *Plasmodium*, is among the most widespread infectious diseases in the world, afflicting several hundred million and killing nearly 2 million people, mainly children, each year (1). The malaria parasite *Plasmodium falciparum* invades erythrocytes and consumes nearly all of its host's hemoglobin as a source of nutrients during growth and development (2). Hemoglobin is catabolized in an acidic digestive vacuole of the parasite. Many of the current antimalarial agents, such as chloroquine, appear to act by disrupting vacuolar functions (3). However, evolution of the ability to prevent vacuolar accumulation of weak bases has led to the emergence of drug-resistant strains of *P. falciparum* (4).

Hemoglobin degradation is mediated by the action of several vacuolar digestive enzymes. A cysteine protease has been identified in *P. falciparum*, based on the fact that cysteine protease inhibitors block the action of a 28-kDa protease and cause accumulation of undigested hemoglobin and parasite death in culture (5). Two aspartic proteases of *P. falciparum* have been implicated in the initial steps of the hemoglobin degradation process (6–8). The first protease, plasmepsin I (Plm I), appears to make a strategic initial cleavage that presumably leads to an unraveling of the native hemoglobin structure such that further proteolysis can rapidly proceed. Plasmepsin II (Plm II), the second aspartic protease, is capable of cleaving native hemoglobin but is more active against denatured or fragmented globin, such as that produced by the action of Plm I. The genes for both plasmepsins have been characterized (6, 8). They encode proteins with sequence homology to mammalian aspartic proteases such as cathepsin D (Cat D) and renin, and are 73% identical to each other. A peptidomimetic inhibitor of Plm I blocks hemoglobin degradation in culture and kills the parasite, validating this pathway as a target for antimalarial drug development (6).

Pepstatin A, a general inhibitor of aspartic proteases of microbial origin (9), was reported to inhibit hemoglobin degradation by extracts of digestive vacuoles of *P. falciparum* (7). Using recombinant Plm II, we have determined the inhibition constant, K_i, for pepstatin A to be 0.006 nM. The high potency of pepstatin A suggests that this compound could serve as an excellent lead for the design of novel and selective antimalarial compounds. To provide a structural framework for subsequent structure-based design, we determined the molecular structure of Plm II in complex with pepstatin A.

MATERIALS AND METHODS

The full proenzyme coding region for Plm II (8) was cloned into pET vector 22B (Novagen) and sequenced in their entirety. Protein was expressed in *Escherichia coli* BL21/DE3, purified from inclusion bodies, refolded, and activated as described (10, 11). Kinetics assays were performed using a fluorogenic substrate, DABCYL-Glu-Arg-Met-Phe-Leu-Ser-Phe-Pro-EDANS, synthesized as described (12). This substrate was designed to mimic the primary hemoglobin cleavage site common to both Plm I and Plm II (7). Kinetics were performed as described (12) and analyzed using a model for tight binding inhibitors (13).

Recombinant Plm II in 100 mM Tris (pH 6.5) was concentrated and then incubated overnight at 4°C with a 10-fold molar excess of pepstatin A dissolved in dimethyl sulfoxide. The final dimethyl sulfoxide concentration was 10%. Crystallization of the complex was performed at 20°C using the vapor-diffusion hanging-drop technique. Drops were prepared by mixing 2 μl of protein-inhibitor solution at approximately 10 mg/ml with an equal volume of reservoir solution containing 0.1 M phosphate buffer (pH 6.5) and 47% $(NH_4)_2SO_4$. Hexagonal rod-shaped crystals appeared within several days; belonged to space group $P3_121$, with $a = b = 104.1$ Å and $c = 97.6$ Å; and contained two molecules in the asymmetric unit. Crystals were transferred to artificial mother liquor containing 25% glycerol. X-ray diffraction data extending to 2.7 Å resolution were collected at −180°C on an imaging plate area detector (Rigaku Co., Japan; model R-AXIS IIC). The x-ray source was a Rigaku RU200 rotating anode generator operating at 50 kV and 100 mA, with a double focusing mirror

The publication costs of this article were defrayed in part by page charge payment. This article must therefore be hereby marked "*advertisement*" in accordance with 18 U.S.C. §1734 solely to indicate this fact.

Abbreviations: Plm I and II, plasmepsins I and II; rmsd, root-mean-square deviation; Cat D, cathepsin D.

Data deposition: The atomic coordinates have been deposited in the Protein Data Bank, Chemistry Department, Brookhaven National Laboratory, Upton, NY 11973 (reference 1SME).

system. A complete data set was collected from two single crystals using a crystal-to-detector distance of 140 mm and exposure times of 40 min for 1.5° oscillations. X-ray diffraction data processing was performed using the programs DENZO (14) and SCALEPACK (15). The data set contained 22,465 unique reflections out of a total of 63,000 measured reflections and was 77% complete to 2.7 Å resolution [$I > 2\,\sigma(I)$]. The overall R_{merge} was 9.4%. The structure was determined by molecular replacement using the program AMORE (16) and the structure of human Cat D (17) as a search model, and was refined using the program XPLOR (18). The refined model includes two protein molecules, two inhibitors, and 115 water molecules. The final R factor is 19.8% for all reflections between 8.0 Å and 2.7 Å after group temperature factor refinement for the protein molecules and individual isotropic temperature factor refinement for inhibitors and water molecules. The deviations of the protein model from ideal geometric parameters are 0.011 Å for bond lengths, 2.1° for bond angles, 26.9° for dihedral angles, and 1.5° for improper angles. The average temperature factors for protein, inhibitor, and solvent molecules are 16.6, 12.5, and 15.4 Å^2, respectively.

RESULTS AND DISCUSSION

The structure of Plm II has the typical bilobal shape and topology of eukaryotic aspartic proteases (Fig. 1) (19). The single chain of 329 amino acids is folded into two topologically similar N- and C-terminal domains related by a pseudo 2-fold rotation axis. The domains contact each other along the bottom of the binding cleft that contains the catalytic dyad, Asp-34 and Asp-214. A β-hairpin structure, known as the "flap," lies perpendicular over the binding cleft and interacts with substrates and inhibitors. The N and C ends of the polypeptide chain of Plm II are assembled into the characteristic six-stranded interdomain β-sheet. Plm II contains two disulfide bridges, Cys^{47}–Cys^{52} and Cys^{249}–Cys^{285}. The latter is conserved among all eukaryotic aspartic proteases, whereas the N-terminal disulfide is conserved only among mammalian enzymes, suggesting a closer evolutionary relationship of the malarial enzymes to their mammalian rather than fungal counterparts. A unique feature of Plm II is the substitution of Ser for Thr at residue 215 in the Asp-Thr-Gly signature sequence for the C domain. Ser has also been observed at this position in some retroviral aspartic proteases that are homodimeric enzymes; however, its functional significance is unclear.

There are two Plm II molecules in the crystallographic asymmetric unit and they do not display the same conformation (Fig. 2). The root-mean-square deviation (rmsd) for the superposition of all 329 corresponding C$^\alpha$ atoms of both molecules is 0.93 Å. Individual superposition of C$^\alpha$ atoms of the N or C domains result in rmsd values of 0.44 Å (266 C$^\alpha$ atoms) and 0.72 Å (40 C$^\alpha$ atoms), respectively‡. Rigid body analysis indicates that the conformations of the two crystallographically independent molecules can be related by a relative rotation of 5.2° between the N and C domains, about an axis approximately passing through C$^\alpha$ atoms of Thr-221 and Gly-291. The translation in the direction of the rotation axis is negligible. After superposition of both molecules on their N-terminal domains, equivalent C$^\alpha$ atoms on the C domain are displaced up to 3.8 Å. Despite these differences, pepstatin A displays the same interactions with the enzyme in both conformations. These two conformational states demonstrate an intrinsic interdomain flexibility of Plm II. In fact, interdomain motion of the magnitude observed here has also been detected in a number of proteins (21). Such flexibility may be important for the ability of Plm II to recognize and bind specific sequences on the native hemoglobin molecule. Previous studies have indicated that hemoglobin degradation proceeds in an ordered fashion with the first cleavage occurring in the native molecule between Phe-33 and Leu-34 in the hinge region of the α chain (7). Prolonged incubation of hemoglobin with purified Plm II results in cleavages between Phe-33/Leu-34, Thr-108/Leu-109 and Leu-136/Thr-137 in the α chain, and Leu-32/Val-33 in the β chain. In the tetrameric form of hemoglobin, none of these sites are surface-accessible. However, the 33/34 site is exposed in the isolated α/β dimer and monomeric forms of hemoglobin which can be favored at the low pH levels within the digestive vacuole (22). Preliminary docking studies suggest that some structural rearrangement of Plm II will be required to facilitate binding of the hinge region of hemoglobin. Different interdomain displacements among the aspartic protease family have been loosely taken as evidence for flexibility of these enzymes and have been proposed to be related to the range of specificity of these enzymes (23–25). The large relative displacements between

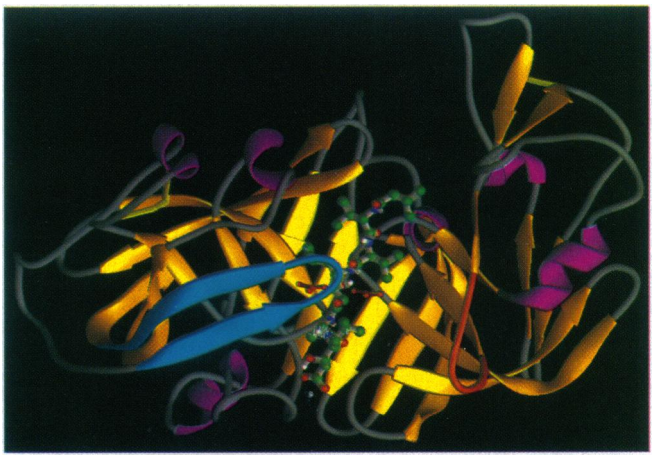

FIG. 1. Ribbon model of Plm II color-coded for secondary structural elements. The β-hairpin "flap" (light blue) and the proline-rich loop (red) are two typical motifs in aspartic proteases. A molecule of pepstatin A, shown in a full atom representation, is at the binding cleft which runs between the homologous N (left) and C (right) domains. The domains interact at the two ψ-loops, which contain the active site Asx residues (side chains in red), and also form a six-stranded antiparallel β-sheet, underneath the active site (yellow arrows parallel to the plane of the paper).

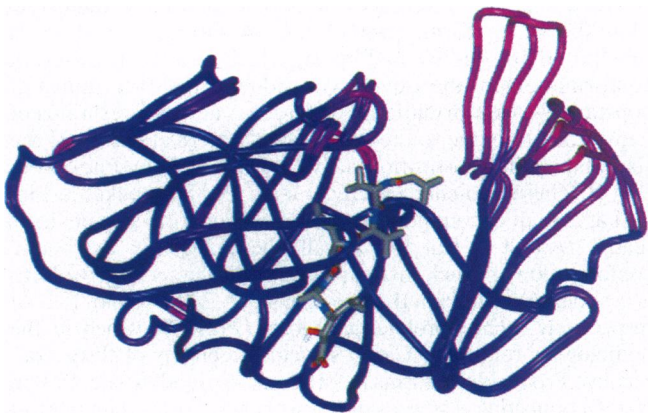

FIG. 2. C$^\alpha$ model of the two conformers of Plm II. The molecules were superimposed using C$^\alpha$ atoms of the N-terminal domain. Distances between equivalent C$^\alpha$ atoms, after the superposition, are color coded blue to red corresponding to the range 0.0–4.0 Å.

‡The superposition of the molecules was done using a McLachlan procedure (20) with an automatic selection of atoms based on the iterative minimization of the function F = rmsd/N, where N is the number of atoms involved in the calculation. An implementation of the method can be found at http://uqbar.ncifcrf.gov.

```
PlmI      NAGDSVTLND     VANV MYYGE     AQIGDNKQKF     AFIFDTGSAN     LWVPSAQCN       TIGCKTKNL
PlmII*001*SSNDNIELND*011*FQNI MFYGD*020*AEVGDNQQPF*030*TFILDTGSAN*040*LWVPSVKCT *049* TAGCLTKNL
          |**|***     |      ||||     ***| | ***     |*||*||***     *******|         |  |*||
Cat D*001* GPIPEVLKN*010*YM DAQYYGE*019*IGIGTPPQCF*029*TVVFDTGSSN*039*LWVPSIHCKL*049*LDIACWIHHK

PlmI      YDSNKSKTYE     KDGTKVEMNY     VSGTVSGFFS     KDIVTIA        NLSFP YKFI      EVTDTNGFEP
PlmII*058*YDSSKSRTYE*068*KDGTKVEMNY*078*VSGTVSGFFS*088*KDLVTVG   *095*NLSLP YKFI*104*EVIDTNGFEP
          |||****|*|     *||*|||*||*     *|*|******     *****|        |*|   |***     ****|    |
Cat D*059*YNSDKSSTYV*069*KNGTSFDIHY*079*GSGSSLSGYLS*089*QDTVSVPCAG*107*GVKVERQVFG*117*EATKQP  GI

PlmI      AYTLGQFDGI     VGLGWKDLSI     GSVDPVVVEL     KNQNKIEQAV     FTFYLPFDDK      H K GYLTIG
PlmII*114*TYTASTFDGI*124*LGLGWKDLSI*134*GSVDPIVVEL*144*KNQNKIENAL*154*FTFYLPVHDK*164*H T GFLTIG
          |||*******     **||||*|*|              |       | ** ||*     ****|           |  *****
Cat D*125*TFIAAKFDGI*135*LGMAYPRISV*145*NNVLPVFDNL*155*MQQKLVDQNI*165*FSFYLSRDPD*175*AQPGGELMLG

PlmI      GIEDRFYEGQ     LTYEKLNHDL     YWQVDLDL H     FGN  LTV E     KATAIVDSGT      SSITAPTEFL
PlmII*172*GIEERFYEGP*182*LTYEKLNHDL*192*YWQITLDA H*201*VGN  IML E*208*KANCIVDSGT*218*SAITVPTDFL
          *| |||****     *|*****||*     |||** |                |***||***      ||** || *|
Cat D*185*GTDSKYYKGS*195*LSYLNVTRKA*205*YWQVHLDQVE*215*VASGLTLCKE*225*GCEAIVDTGT*235*SLMVGPVDEV

PlmI      NKFFEGLDVV     KIPFLPLYIT       TCNNPKLP     TLEFR SATN     VYTLEPEYYL      QQIFDFGISL
PlmII*228*NKMLQNLDVI*238*KVPFLPFYVT*248*  LCNNSKLP*256*TFEFT SENG*265*KYTLEPEYYL*275*QHIEDVGPGL
                                                     |              |||||
Cat D*245*RELQKAIGAV*255*PLIQGEYMIP*265*CEKVST  LP*273*AITLKLGG K*282*GYKLSPEDYT*292*LKVSQAGKTL

PlmI      CMVSIIPVDL          NKNTFI     LGDPFMRKYF     TVFDYDNHTV     GFALAKKKL
PlmII*285*CMLNIIGLDF*295*     PVPTFI*301*LGDPFMRKYF*311*TVFDYDNHSV*321*GIALAKKNL
          * |||||               |**     **|***|***     **********     ****|*
Cat D*302*CLSGFMGMDI*312*PPPSGP LWI*321*LGDVFIGRYY*331*TVFDRDNNRV*341*GFAEAA
```

FIG. 3. Structure-based alignment of the amino acid sequences of Plm I, Plm II, and human Cat D. The structural alignment between Plm II, in closed conformation between the C and N domains, and Cat D was performed in two steps. First, the amino acid sequences were aligned according to the conserved amino acids, and the C^{α} atoms of those pairs were superimposed. Then, in an iterative procedure, all C^{α} atom pairs closer than 1.5 Å were used to compute the superposition transformation, the molecules were superimposed, and pairs closer than 1.5 Å were computed again. The process was finished when the number of distance-equivalenced pairs remained constant. There are 212 pairs of equivalent C^{α} atoms at a distance less than 1.5 Å (rmsd = 0.7 Å) and 126 at a distance less than 0.75 Å (rmsd = 0.49). The vertical bars between Plm II and Cat D sequences indicate pairs closer than 1.5 Å, and the stars indicate pairs closer than 0.75 Å. The rmsd for all 318 pairs in the alignment is 1.97 Å, and 126 pairs correspond to conserved amino acids. Plm I and Plm II sequences were aligned by matching conserved amino acids.

domains of the two crystallographically independent Plm II molecules observed here provide direct evidence of the segmental mobility of this enzyme.

Plm II has a high sequence homology with mammalian aspartic proteases. In particular, its highest homology is with human Cat D; they have 116 amino acids in common or 35% identity (Fig. 3). However, a considerably higher degree of homology at the active sites is evident upon structural comparison of the pepstatin A complexes of Plm II and Cat D (17) (Fig. 4 *A* and *B*), and a few significant changes are balanced. For instance, Gly-79 in Cat D, at the tip of the flap, has been replaced by Val-78 in Plm II. A compensating substitution from the C-domain region, Met-309 in Cat D for Leu-292 in Plm II, keeps the narrowest section of the binding cleft at the same width, 4.7 Å, as measured between closest side chain carbon atoms. Phe-126 in Cat D at the S1 site[§] has been substituted by Phe-111 in Plm II. That is, despite the fact that these amino acids do not occupy equivalent positions on the sequence or in the structural alignment (Fig. 3), their phenyl rings form the same binding subsite. The central part of pepstatin A is bound in a similar manner to Cat D and to Plm II, but there are differences at both ends of the molecule. Met-307, which forms part of the S4 subsite in Cat D, is substituted by Ile-290 in Plm II, which results in different conformations of the isovaleryl residue at the N terminus of pepstatin A. Conformational differences at the C terminus of pepstatin A are due to the presence of Val-78 at the tip of the flap and to the substitution of Ile-311 in Cat D by Phe-294 in Plm II. These two changes create a smaller S3′ pocket in Plm II that cannot accommodate the terminal statine side chain as readily as that in Cat D. Overall, the changes in the bound conformation are such that pepstatin A displays a larger solvent accessible area in Plm II than in Cat D, 289 $Å^2$ and 182 $Å^2$ respectively[¶]. The "proline-rich" loop (292–300) which in the homologous renin and Cat D structures consists of three consecutive Pro residues, forms a portion of the binding site. In Plm II, the connecting β-strands of this loop are shorter than in most aspartic proteases, and the loop contains only two Pro residues separated by a Val residue. Unlike in Cat D (17) and renin (28), both of the Pro residues participate in trans peptide linkages.

The homology between the plasmepsins and Cat D prompted us to investigate whether cross-inhibition would be observed with a panel of linear and cyclic inhibitors of Cat D which contain modified statine motifs (unpublished data). Compounds 1–5 (Fig. 5), which have inhibition constants ranging from 0.02 to 1.4 nM for Cat D, were chosen to reflect a wide range of predicted relative binding affinities for Plm II based on preliminary docking experiments. Measured K_i values range from 0.04 to 1500 nM for Plm II (Fig. 5). The linear compounds 1–3 are based on the structure of pepstatin A, with a 4(s)-amino-3(s)-hydroxy-5-phenylpentanoic acid rather than a statine motif at the P1-P1′ positions. Compound 1 has the highest similarity with pepstatin A and is the best of the three linear inhibitors, both for Cat D and Plm II. Compound 4, which contains an 8 atom bridge between the P3 and P1 positions, is a subnanomolar inhibitor of Plm II, as well as of Cat D. The S3 and S1 subsites are contiguous and relatively unobstructed in both enzymes and thus afford cyclization strategies for inhibitor design. The P2-P3′ bridged compound 5, which was included in the test panel as a negative control, is a weak inhibitor of Plm II. Modeling analysis suggests that the side chain of Val-78 in Plm II, at the tip of the flap, would interfere with the binding of the cyclic portion of this compounds.

Despite the nanomolar to sub-nanomolar inhibitory potency of compounds 1–4 with Plm II, only compound 1 exhibited antimalarial activity in cell culture assays (Fig. 5). Based on Fig. 5 and structural models of the docked inhibitors with Plm II and Cat D, inhibitors 6–8 were designed to improve solubility and cell penetrability. A key feature of these compounds is their smaller size, which results in some loss of enzyme inhibitory potency. The most potent compound against Plm II, compound 7, is also the best inhibitor of *P. falciparum* in culture. Another interesting aspect of these compounds is their improved specificity toward Plm II. That is,

[§]The nomenclature of Schechter and Berger (26) is used to describe the locations, P-P′, of side-chain substituents of the inhibitor and the corresponding S-S′ subsites, or binding pockets, in the enzyme.

[¶]Solvent-accessible areas were computed using the program M (27), with a 1.8 Å radius probe. M and a discussion of the surface area algorithm are available at http://uqbar.ncifcrf.gov.

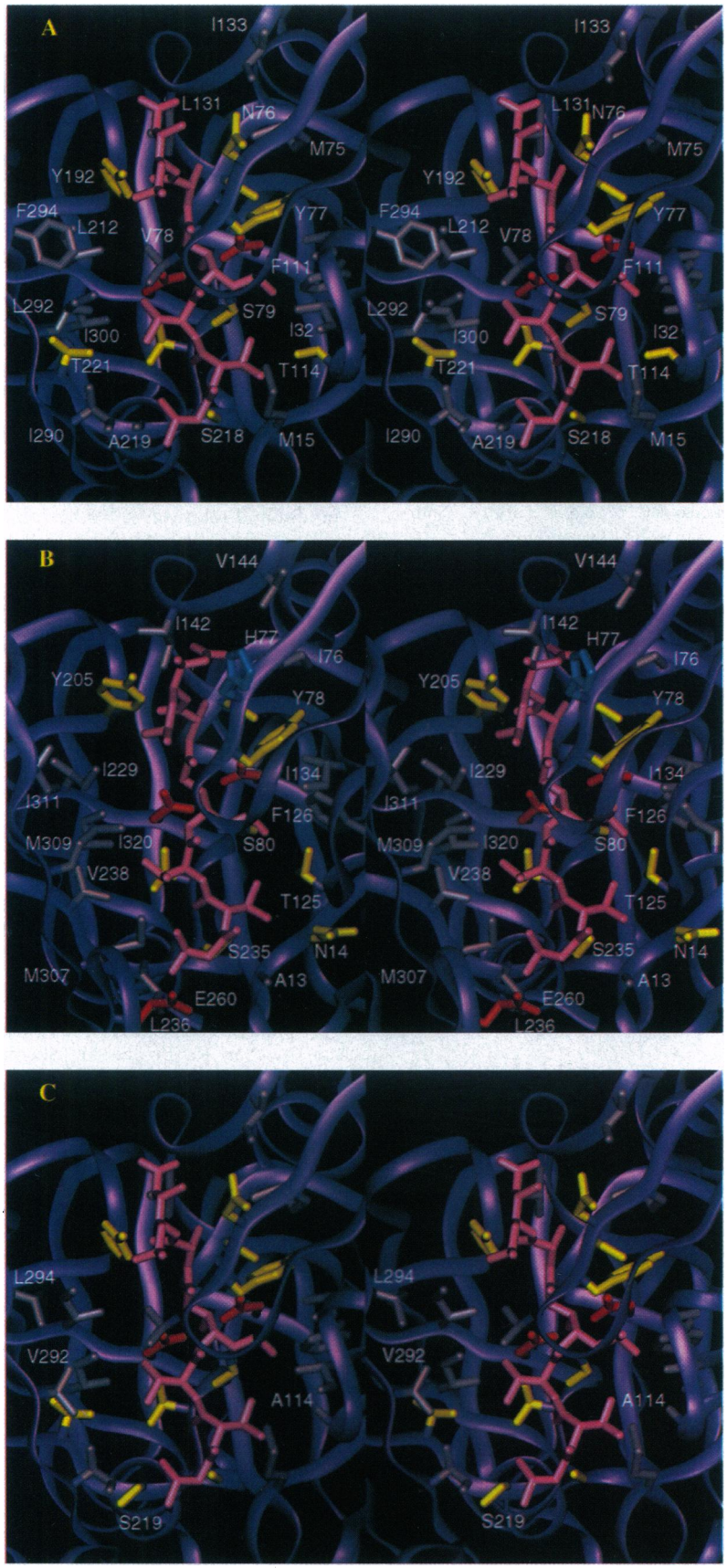

FIG. 4. Stereoview of binding clefts. Pepstatin A is in pink and side chains are color coded according to their polarity: gray for hydrophobic, yellow for polar, red for acidic, and blue for basic. Note the active site Asp residues in the center of each figure and below the tip of the flap, interacting with a statine hydroxyl. Plm II (*A*), Cat D (*B*), and Plm I (*C*) model-built by homology to the Plm II structure. Only side chains that differ from Plm II have been labeled.

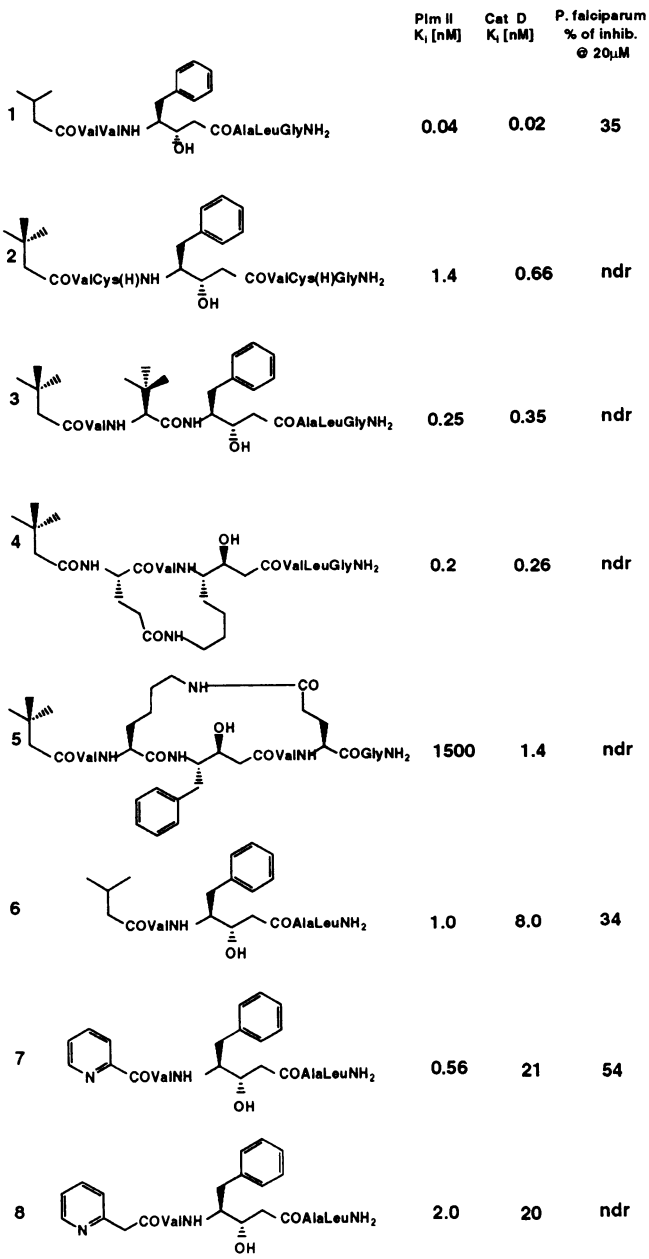

FIG. 5. Inhibition of Plm II, human Cat D, and *P. falciparum* growth in a human erythrocyte assay. Inhibition constants, K_i, were measured as described in the text. Growth inhibition of *P. falciparum* clone HB-3 trophozoites in human erythrocytes was measured by an hypoxanthine incorporation assay as described (6).

whereas compounds 1–4, which were designed using the Cat D structure, have similar inhibitory potency toward Cat D and Plm II, compounds 6–8 are, on average, 20 times more potent toward Plm II than toward Cat D.

The structures of Plm II and its homology-modeled relative, Plm I,[‖] reveal highly homologous active sites (Fig. 4 *A* and *C*), which explains their similar cleavage site preferences (7). Only three amino acid differences that would directly affect a pepstatin-like inhibitor were observed between the binding clefts. Phe-294 in Plm II becomes Leu in Plm I, creating a larger S3′ pocket in the latter, similar to that observed in Cat D. Also, Leu-292 in Plm II, which together with Val-78 closes the binding cleft around pepstatin A, becomes Val in Plm I, thus generating a binding cleft slightly more open than that in either Cat D or Plm II. The third substitution is Thr-114 in Plm II for Ala-114 in Plm I, which creates a larger and more hydrophobic S3 subsite in Plm I. These few differences between Plm I and Plm II, at the binding cleft, suggest that pepstatin A should bind in a similar manner to both enzymes.

Our results provide a structural framework for the design of selective inhibitors of plasmepsins and, somewhat unexpectedly, provide direct experimental evidence for interdomain flexibility. Previous comparative studies of aspartic proteases in different crystal forms have indicated a minor degree of conformational flexibility in these enzymes (23). However, the magnitude of the subdomain displacement seen for Plm II in the same crystal is much larger than these examples and places new limits on subdomain movement in these enzymes. Structural differences in the active sites of Plm II and Cat D were used to rationalize differential inhibition of these enzymes and can be exploited for drug design. The demonstration that potent and relatively selective inhibitors of Plm II also inhibit the growth of *P. falciparum* in cell culture strongly supports the concept that inhibition of plasmepsins is a viable strategy for antimalarial therapy.

We thank Mrs. Betty Yu for excellent technical assistance. This research was supported in part by the National Cancer Institute under contract NOl CO-56000; by National Institutes of Health Grant AI 37977 to D.E.G., who is a Charles E. Culpepper Medical Scholar; and by the United Nations Development Program/WORLDBANK/World Health Organization Special Programme for Research in Tropical Diseases.

1. Sturchler, D. (1989) *Parasitol. Today* **5,** 39–40.
2. Scheibel, L. W. & Sherman, I. W. (1988) in *Malaria*, eds. Wernsdofer, W. H. & McGregor, I. (Churchill Livingstone, London), pp. 219–252.
3. Olliaro, P. I. & Goldberg, D. E. (1995) *Parasitol. Today* **11,** 294–297.
4. Slater, A. F. G. (1993) *Pharmacol. Ther.* **57,** 203–235.
5. Rosenthal, P. J., Wollish, W. S., Palmer, J. T. & Rasnick, D. (1991) *J. Clin. Invest.* **88,** 1467–1472.
6. Francis, S. E., Gluzman, I. Y., Oksman, A., Knickerbocker, A., Mueller, R., Bryant, M., Sherman, D. R., Russell, D. G. & Goldberg, D. E. (1994) *EMBO J.* **13,** 306–317.
7. Gluzman, I. Y., Francis, S. E., Oksman, A., Smith, C. E., Duffin, K. L. & Goldberg, D. E. (1994) *J. Clin. Invest.* **93,** 1602–1608.
8. Dame, J. B., Reddy, G. R., G., Yowell, C. A., Dunn, B. M., Kay, J. & Berry, C. (1994) *Mol. Biochem. Parasitol.* **64,** 177–190.
9. Umezawa, H., Aoyagi, T., Morishima, H., Matsuzaki, M., Hamada, M. & Takeuchi, T. (1970) *J. Antibiot. (Tokyo)* **23,** 259–262.
10. Hill, J., Tyas, L., Phylip, L. H., Kay, J., Dunn, B. M. & Berry, C. (1994) *FEBS Lett.* **352,** 155–158.
11. Luker, K. L., Francis, S. E., Gluzman, I. Y. & Goldberg, D. E. (1996) *Mol. Biochem. Parasitol.*, in press.
12. Matayoshi, E. D., Wang, G. T., Krafft, G. A. & Erickson, J. (1990) *Science* **247,** 954–958.
13. William, J. W. & Morrison, J. F. (1979) *Methods Enzymol.* **63,** 437–467.
14. Otwinowski, Z. (1993) DENZO: An Oscillation Data Processing Program for Macromolecular Crystallography (Yale Univ. Press, New Haven, CT).
15. Otwinowski, Z. (1993) SCALEPACK: Software for the Scaling Together of Integrated Intensities Measured on a Number of Separate Diffraction Images (Yale Univ. Press, New Haven, CT).
16. Navaza, J. (1994) *Acta Crystallogr. A* **50,** 157–163.
17. Baldwin, E. T., Bhat, T. N., Gulnik, S., Hosur, M. V., Sowder, R. C., Cachau, R. E., Collins, J., Silva, A. M. & Erickson, J. W. (1993) *Proc. Natl. Acad. Sci. USA* **90,** 6796–6800.
18. Brünger, A. T., (1992) X-PLOR: A System for X-ray Crystallography and NMR (Yale Univ. Press, New Haven, CT), Version 3.1.

[‖]A full model of Plm I was built based on the structure of Plm II, by substitution of non-identical side-chains using the program QUANTA (Molecular Simulations, Inc.). Only the orientation of substituted side-chains was optimized.

19. Davies, D. (1990) *Annu. Rev. Biophys. Biophys. Chem.* **19,** 189–215.
20. Diamond, R. (1976) *Acta Crystallogr. A* **32,** 1–10.
21. Gerstein, M., Lesk, A. M. & Chothia, C. (1994) *Biochemistry* **33,** 6739–6749.
22. Chu, A. H. & Ackers, G. K. (1981) *J. Biol. Chem.* **256,** 1199–1205.
23. Erickson, J. W., Baldwin, E. T., Bhat, T. N. & Gulnik, S. (1995) in *Aspartic Proteinases: Structure, Function, Biology and Biomedical Implications*, ed. Takahashi, K. (Plenum, New York), pp. 181–192.
24. Abad-Zapatero, C., Rydel, T. J. & Erickson, J. W. (1990) *Proteins* **8,** 62–81.
25. Sali, A., Veerapandi, J. B., Cooper, S. I., Foundling, S. I., Hoover, D. J. & Blundel, T. L. (1987) *EMBO J.* **8,** 2179–2188.
26. Schechter, I. & Berger, A. (1967) *Biochem. Biophys. Res. Commun.* **27,** 157–163.
27. Cachau, R. E. (1994) *Biophys. Chem.* **51,** 1–17.
28. Sielicki, A. R., Hayakawa, K., Fujinaga, M., Murphy, E. P., Fraser, M., Muir, A. K., Carilli, C. T., Lewicki, J. A., Baxter, J. D. & James, M. N. G., (1989) *Science* **243,** 1346–1351.